

Rietveld analysis of the modulated structure in the superconducting oxide $\text{Bi}_2(\text{Sr,Ca})_3\text{Cu}_2\text{O}_{8+x}$

Akiji Yamamoto, Mitsuko Onoda, Eiji Takayama-Muromachi, and Fujio Izumi
National Institute for Research in Inorganic Materials, Tsukuba 305, Japan

Tōru Ishigaki and Hajime Asano
Institute of Materials Science, University of Tsukuba, Tsukuba 305, Japan
(Received 16 June 1989; revised manuscript received 27 December 1989)

The modulated structure of the high- T_c superconductor $\text{Bi}_2(\text{Sr,Ca})_3\text{Cu}_2\text{O}_{8+x}$ was analyzed with a newly developed Rietveld refinement program for modulated structures. The structure refinement was made by the simultaneous refinement method using x-ray and time-of-flight neutron-diffraction data. It has a one-dimensionally modulated structure with $N Bbmb/1\bar{1}1$, $a = 5.3957(3)$, $b = 5.3971(3)$, $c = 30.649(1)$ Å, and $\mathbf{k} = 0.2118(1)\mathbf{b}^*$. Atoms in Bi-O, Sr-O, Cu-O, and Ca layers are all greatly displaced from their average positions. In particular Bi atoms are displaced mainly along the b axis, forming Bi-condensed and Bi-dilute regions. The characteristic feature of the structure is the existence of extra oxygens, giving $x = 1.0$, in the Bi-dilute region of the Bi-O layer. Bi has a distorted rocksalt-type oxygen coordination with four short Bi—O bonds in the Bi-condensed region and a deformed square pyramidal coordination with five Bi—O bonds in the Bi-dilute region. The apical oxygen of a CuO_5 pyramid, which joins Cu to Bi, moves along with Bi, distorting the pyramid considerably.

I. INTRODUCTION

The high- T_c superconducting oxides $\text{Bi}_2(\text{Sr,Ca})_3\text{Cu}_2\text{O}_{8+x}$ and $\text{Bi}_2\text{Sr}_2\text{CuO}_{6+x}$ are known to have incommensurate modulated structures.¹⁻⁶ The average structure of the former has been determined using x-ray diffraction,³⁻⁶ and an x-ray analysis using single-crystal diffraction has been attempted to determine the modulation of metal atoms.⁷ It was also shown using the thermogravimetry and chemical analysis that extra oxygen atoms giving $x > 0$ exist.^{3,6} The extra oxygen creates the holes that are considered to be responsible for superconductivity and is therefore important for understanding the mechanism of superconductivity. The large absorption coefficient due to Bi and platy crystal habits, however, does not facilitate the detailed analysis of the incommensurate structure using single-crystal x-ray diffraction. Consequently, neither the modulation waves of oxygens nor the position of the extra oxygen have been given. Neutron scattering is known to be quite suitable for the refinement of structure parameters for oxygen even under the presence of heavy atoms. Unfortunately a sufficient single-crystal size for neutron analysis has not been obtained because of the difficulty in its crystal growth.

The modulated-structure analysis of $\text{Bi}_2\text{Sr}_2\text{CuO}_{6+x}$ using the x-ray single-crystal method has been made with the commensurate approximation for a nearly commensurate case.⁸ This compound has, in general, an incommensurate modulated structure though it becomes nearly commensurate under some conditions. The structure is believed to have no extra oxygen (i.e., $x = 0$). Since the extra oxygen plays an essential role in superconductivity,

it will be important to examine this problem using neutron diffraction.

These two are key compounds for understanding the structures of superconducting Bi-Tl compounds. The purpose of the present work is the determination of these two structures by the combined use of x-ray and neutron-powder-diffraction methods. This paper deals with the title compound.

Soon after the discovery of $\text{Bi}_2(\text{Sr,Ca})_3\text{Cu}_2\text{O}_{8+x}$, electron microscopy clarified the existence of Bi rich and poor regions that are parallel to the a axis of the orthorhombic average structure.⁹ The average structure has 4 formula units (f.u.) in the pseudotetragonal cell with $a = b = 5.40$ Å and $c = 30.7$ Å. The Bi-rich regions are arranged with a period of about $4.8b$, which is incommensurate with b . The displacive and occupational-substitutional modulations of the metal atoms are examined based on the simulation of a structure image.¹⁰ Bi atoms are largely displaced along the b axis, while Ca and Cu mainly shift along the c axis. Sr has an intermediate character between these two. For all of the metal atoms, the displacements are almost sinusoidal. The analyses also suggest the existence of the strong substitutional modulation at the metal sites, but this is not consistent with the result of x-ray diffraction.⁷

The average structure has been analyzed using single-crystal x-ray diffraction.³⁻⁶ It determined metal and most oxygen positions. There are, however, several models for the arrangement of oxygen atoms on the Bi-O plane. Because of the difficulty in determining oxygen positions under the existence of heavy atoms, the discrepancies still remain in the models proposed so far on the basis of x-ray and neutron diffraction data and electron microscopy.^{3-6,10-13} The coordination of oxy-

gen atoms around Bi in these models are roughly classified into three groups: octahedral coordination (rocksalt type),³⁻⁶ square pyramidal coordination (oxygen-deficient perovskite type),¹¹ and the mixture of these two.¹³ The second and third types introduce extra oxygen atoms, giving $x = 2$ and $0 < x < 2$, respectively.

Clear evidence for the existence of the extra oxygens has been shown not for $\text{Bi}_2(\text{Sr,Ca})_3\text{Cu}_2\text{O}_{8+x}$ but for isostructural $\text{Bi}_2(\text{Sr,Y})_3\text{Cu}_2\text{O}_{8+x}$ by single-crystal x-ray and neutron powder diffraction.¹⁴ The detailed average structure analysis of $\text{Bi}_2(\text{Sr,Y})_3\text{Cu}_2\text{O}_{8+x}$ showed that the extra oxygen atoms with $x = 0.7$ exist in the Bi-O layer, constructing the distorted pyramidal coordination around Bi. Furthermore, Bi and O in this layer and the apical oxygen of the CuO_5 square pyramid require a split atom approximation, which indicates that the atoms move largely around the average position or take two positions with occupation probabilities less than 1. Because of the limitation of the average structure analysis, the local arrangement of atoms remains unknown. The analysis of the modulated structure is needed to obtain detailed information on the structure of $\text{Bi}_2(\text{Sr,Ca})_3\text{Cu}_2\text{O}_{8+x}$.

The above results suggest two models for the modulation in the Bi-O layer: displacive and occupational modulation. In order to clarify the modulation including that of the oxygen atoms, we need neutron-diffraction data. In the present paper, powder diffraction is used in the respect that specimen preparation and a diffraction experiment are quite easy. Fortunately satellite intensities are strong enough to be detected by the powder method in the present case. It has, however, a serious weak point for the analysis of a complicated structure: information contained in powder data is poor compared with the single-crystal method. Many reflection profiles overlap in the diffraction pattern of a complicated structure like the present case. As a result, we cannot get the individual intensity for each reflection. Even if we use Rietveld analysis, heavily overlapped peaks may give poor information about the modulated structure. In order to complement the weak point, we use x-ray and neutron powder diffraction data and the penalty function method. As is well known, neutron scattering is quite adequate for determining oxygen positions when the structure includes heavy atoms, while heavy-atom positions are well defined by x-ray scattering. Furthermore, it is favorable to use simultaneous refinement of these data because the structural parameters should be the same in the two analyses, but individual refinements give more or less different results. The penalty function method is effective to restrain the appearance of crystallochemically unreasonable structures in the refinement.

There had been no Rietveld refinement program for the modulated structure, though such programs have been developed for single-crystal data. Therefore we developed a new program for the present purpose, modifying an existing refinement program for the single-crystal method. We employed the time-of-flight (TOF) method for neutron powder diffraction and the conventional angle-dispersive method for x-ray scattering. The program is, however, designed so as to be applicable to the analysis with any combination of angle-dispersive x-

ray and/or neutron data and neutron data taken on a high-resolution TOF powder diffractometer (HRP) at the National Laboratory for High Energy Physics (KEK). It is extended from the existing program REMOS for the refinement of modulated structures with a single crystal.¹⁵ It inherits a variety of features from REMOS, which in particular employs the penalty function method to restrict structural parameters within reasonable ranges.¹⁶ For profile shape functions, we used those adopted in RIETAN.¹⁷ A detailed description of the program is planned to be published elsewhere.

The program has been successfully applied to the modulated structure of the title compound. It shows strong satellite intensities, and all of the reflections are indexable with four indices $h, k, l,$ and m by $q = ha^* + kb^* + lc^* + mk$, where $k \approx 0.21b^*$ and q is a diffraction vector.¹⁸ The symmetry of such a structure is designated by a superspace group. From the systematic extinction rules observed in electron-diffraction patterns, a possible superspace group is $N Bbmb/1\bar{1}1$ or its subgroup $N Bb2b/111$.^{13,18,19} The average structure has a large unit cell including 4 f.u. in it. Consequently, the model with the latter superspace group includes so many parameters that Rietveld analysis is difficult. In the present analysis, therefore, we assume the former. The present analysis clarifies the whole modulation including that of the oxygen atoms and shows the existence of the extra oxygens inserted in the Bi-O layer with the periodicity of the modulation wave.

The arrangement of this paper is as follows. In Sec. II, we describe sample preparation and x-ray and neutron-diffraction experiments. The refinement method and possible models are discussed in Sec. III. The results of the refinement are shown in Sec. IV. In Sec. V we check several other possibilities of the origin of the modulation proposed so far.

II. EXPERIMENTAL

The powder specimen of the title compound was prepared by solid-state reaction using Bi_2O_3 , SrCO_3 , CaCO_3 , and CuO as starting reagents. A mixture having the nominal composition of $\text{Bi}_4\text{Sr}_3\text{Ca}_3\text{Cu}_4\text{O}_y$ was calcined at 800°C for 1 day and then heated at 850°C in an atmosphere of O_2 for 5 days with a few intermediate grindings.²⁰

Neutron-diffraction data were taken on the high-resolution TOF neutron powder diffractometer (HRP) at the KENS pulsed spallation neutron source at the National Laboratory for High Energy Physics (KEK), while x-ray data were collected using a Rigaku RAD-RB diffractometer equipped with a curved graphite monochromator with $\text{Cu } K\alpha$ radiation. The full width at half maximum (FWHM) depends a little on samples because this material includes planar intergrowths of other phases with different c values and their contents are slightly different from sample to sample. This causes a serious problem in Rietveld analysis because the FWHM of each line varies irregularly, depending on the indices $h, k, l,$ and m , and it is impossible to correct such an anisotropic change in the Rietveld refinement program. The in-

clusion of the intergrowths generally increases the FWHM. The sample used is of lower intergrowth content than several other samples prepared under slightly different conditions, but includes a trace amount of Ca_2CuO_3 and CaO .

III. REFINEMENT METHOD AND MODEL CONSTRUCTION

We can use the Rietveld refinement method, which is quite similar to that employed in REMOS for the present purpose.^{15,16} In REMOS, the summation of the squared weighted R factor (R_w)² and the squared penalty functions P^2 is minimized by the least-squares method. In the present case, R_w is replaced by the weighted pattern R factor (R_{wp}). If we employ several data sets in an analysis, the summation of (R_{wp})² over all the data sets can be used instead of a single (R_{wp})². For the profile functions, we follow RIETAN,¹⁷ in which the pseudo-Voigt function is used in the angle-dispersive method (for both x-ray and thermal neutron diffraction), while it is the concatenation of two Gaussian and one exponential function in the TOF neutron diffraction (some profile parameters are, however, modified from those of RIETAN). The preferred orientation factor is given by $p_1 + (1-p_1)p_2(\pi/2)^2 \exp(\phi) / [1 - \exp(\pi/2)]$, where $\exp(\phi) = \exp(-p_2\phi^2)$, ϕ is the angle between the diffraction vector and the preferred orientation direction (in radian) and p_1 and p_2 are refinable parameters.

The modulated structure is refined in the present analysis together with the average structure based on several models and the superspace group $N Bbmb / \bar{1}11$. This is because the independent refinement of the average structure is difficult in the present case. Many satellite reflections are overlapped with the main reflections in the diffraction patterns. This makes it impossible to refine the structure with two steps (the refinements of the average structure and modulated structure) as in the single-crystal method because the average structure analysis needs intensities only from the main reflections.

The fundamental structure assumed in the analysis is shown in Fig. 1 and Table I. This structure has octahedral oxygen coordination around Bi [O(3) and O(4)] or square-pyramidal coordination [O(3), O(5), and O(6)] but O(4)–O(6) are partly deficient because of the occupational modulation. In preliminary simulations using neutron-diffraction data,¹² we checked three models, in which Bi has octahedral coordination, square-pyramidal coordination, and a mixture of these two, together with many other oxygen arrangements. The best result was obtained from the third model. This implies the existence of the extra oxygen atoms with $0 < x < 2$ in the chemical formula. In this stage, we employed two models taking into account the extra oxygen atoms; these two are slightly different from each other. In the first model (model 1), we consider all the oxygen atoms from O(1) to O(6) in Table I, but O(4) and O(5) plus O(6) are assumed to exist with the occupation probability of p and $1-p$, respectively, while in the second model (model 2), O(4) is deleted and O(5) and O(6) are assumed to be partly occupied. The former gave a more reasonable result with a smaller R factor and without too short Bi–O distances

than the latter. (The final R_{wp} factors for the neutron data were 0.092 in model 1 and 0.107 in model 2.) The refinement based on model 1 will hereafter be described. In this model, there are two competing types of planar arrangements of oxygen atoms in the Bi–O layer.

Under the superspace group $N Bbmb / \bar{1}11$, all the atoms are at the special positions. Then the modulation functions are restricted in their shape owing to the requirement of the site symmetry. The Wyckoff position $8l(x, \frac{1}{2}, z)$ in $Bbmb$ is invariant under the site symmetry group generated by $(\sigma_y | 0, 0, 0)$. The string atom in the four-dimensional crystal at this position should be invariant under the site symmetry group generated by the corresponding symmetry element $(\sigma_y | 0, 0, 0, 0)$ in the superspace group.²¹ The allowed modulation function is ob-

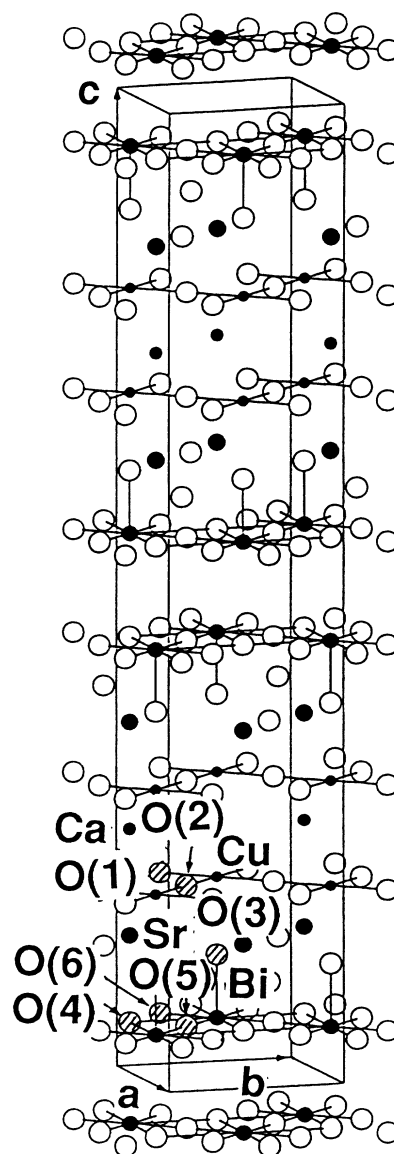


FIG. 1. The fundamental structure used in the refinement. In the Bi–O layer, the O(4)–O(6) sites are occupied with the occupation probability of $\frac{1}{2}$. Solid and open circles represent metal and oxygen atoms.

TABLE I. The structural parameters of the fundamental structure.

Atom	Wyckoff position	x	y	z	p
Bi	8l	0.25	0.5	0.0528	1.0
Sr	8l	0.25	0.0	0.1409	1.0
Ca	4e	0.25	0.0	0.25	1.0
Cu	8l	0.25	0.5	0.1963	1.0
O(1)	8g	0.0	0.25	0.1963	1.0
O(2)	8g	0.5	0.25	0.1963	1.0
O(3)	8l	0.25	0.5	0.1170	1.0
O(4)	8l	0.25	0.0	0.0528	0.5
O(5)	8g	0.5	0.25	0.0528	0.5
O(6)	8g	0.0	0.25	0.0528	0.5

tained by solving

$$(\sigma_y|0,0,0,0)\mathbf{u}(t)=\mathbf{u}(t), \quad (1)$$

where $\mathbf{u}(t)$ is the displacement vector from the position in the fundamental structure, which is a periodic function of $t=\mathbf{k}\cdot(\bar{\mathbf{x}}+\mathbf{X})$. The wave vector of the modulation wave \mathbf{k} is about $0.21\mathbf{b}^*$ in the present case (which is refined together with the lattice constants), $\bar{\mathbf{x}}$ stands for the atom position in the fundamental structure, and \mathbf{X} is a lattice vector. The atom at $\bar{\mathbf{x}}+\mathbf{X}$ in the fundamental structure moves to $\bar{\mathbf{x}}+\mathbf{X}+\mathbf{u}(t)$ owing to the modulation. The phase of the modulation wave t corresponds to the fourth coordinate in the four-dimensional description of the modulated structure. The displacement vector is expressed in terms of the Fourier series as

$$\mathbf{u}(t)=\sum_n \mathbf{u}_n \cos(2\pi n t) + \mathbf{v}_n \sin(2\pi n t), \quad (2)$$

with the n th order Fourier amplitude of \mathbf{u}_n and \mathbf{v}_n . Since a rotation operator R in the symmetry operator of the superspace group transforms the vector field $\mathbf{u}(t)$ into $R\mathbf{u}(\pm t)$ when $R\mathbf{k}=\pm\mathbf{k}$, the operator $(\sigma_y|0,0,0,0)$ transforms $u_i(t)$ into $u_i(-t)$ for $i=1$ and 3 and $u_2(t)$ into $-u_2(-t)$, where $i=1, 2,$ and 3 represents the $\mathbf{a}, \mathbf{b},$ and \mathbf{c} components. Equations (1) and (2) lead to $v_{1n}=v_{3n}=0$, $u_{2n}=0$ for any n . Therefore cosine wave is possible for the \mathbf{a} and \mathbf{c} components and sine wave for the \mathbf{b} component. The site symmetry also requires

$$(\sigma_y|0,0,0,0)p(t)=p(t) \quad (3)$$

for the occupation probability $p(t)$. The rotation operator plays no role for the scalar. Therefore $(\sigma_y|0,0,0,0)$ transforms $p(t)$ into $p(-t)$. This concludes that only the cosine wave is possible for the occupation probability. In the present case Bi, Sr, Cu, O(3), and O(4) take the Wyckoff position 8l. The remaining atoms are at the Wyckoff positions 4e (Ca) and 8g [O(1), O(2), O(5), and O(6)] (see Table I). Similar considerations lead to possible modulation waves for these atoms. The result is shown in Table II. It is noted that the first-order Fourier amplitude of the Ca site should be zero for the displacement along the b direction and for the occupation probability because of its site symmetry.

The modulated structure is refined by taking the Fourier amplitudes as parameters. The harmonic ap-

proximation is used in the analysis because the second-order satellite reflections seem to be weak in electron diffraction and x-ray powder patterns. The structure factors are, however, calculated up to the second-order satellites in order to take into account the diffraction harmonics. This is important when the displacive modulation is strong as in the present case and when intensities up to high- Q values are used. The harmonic modulation causes the higher-order satellite reflections particularly in higher- Q regions. In neutron diffraction, the intensity is strong up to higher- Q values compared with x-ray diffraction because the scattering length is independent of Q . We use intensity data with the diffraction vector $Q=2\pi q$ up to 9 \AA^{-1} . In such a case many second-order satellite reflections have the same order of intensities as the first-order satellites.

In the harmonic approximation there exist 47 positional parameters, of which 14 parameters are the zeroth-order Fourier amplitudes representing the deviation of the average structure from the fundamental structure we assumed. The number of occupational parameters depends on the model. For the occupational and/or substitutional modulations, we can consider several possibilities. The refinement of the occupation probabilities of the Sr and Ca sites showed that the former is nearly 1 and the latter greater than 1, indicating that the Ca site is partly occupied by heavy atoms (the order of scattering

TABLE II. Possible Fourier terms for the displacement and the occupation probability in each Wyckoff position. The zeroth-order Fourier term is represented by 1.

Wyckoff position		Fourier terms	
8l	x	1	$\cos(2\pi t)$
	y		$\sin(2\pi t)$
	z	1	$\cos(2\pi t)$
	p	1	$\cos(2\pi t)$
8g	x		$\sin(2\pi t)$
	y		$\sin(2\pi t)$
	z	1	$\cos(2\pi t)$
	p	1	$\cos(2\pi t)$
4e	x		$\cos(2\pi t)$
	y		
	z		$\cos(2\pi t)$
	p	1	

TABLE III. Allowed ranges of the Cu—O and Bi—O lengths in the penalty function. $O(i)^j$ means the atom obtained from $O(i)$ by the j th symmetry operation.

Bond	Range (Å)	Bond	Range (Å)
Bi—O(3)	2.0–3.5	Cu—O(1)	1.8–3.5
Bi—O(5)	2.0–3.5	Cu—O(1) ^b	1.8–3.5
Bi—O(5) ^a	2.0–3.5	Cu—O(2)	1.8–3.5
Bi—O(6)	2.0–3.5	Cu—O(2) ^a	1.8–3.5
Bi—O(6) ^b	2.0–3.5	Cu—O(3)	1.8–3.5

^a $-x + 1, y + \frac{1}{2}, z$.

^b $-x, y + \frac{1}{2}, z$.

lengths for Bi, Sr, and Ca in neutron scattering is the same as that of their structure factors in x-ray scattering). It can be considered that the Ca site is partly replaced by Bi and/or Sr. In both cases, the Sr/Ca ratio is greater than 2. It is also possible to consider that the Sr site is partly occupied by Ca and Bi because Ca and Bi with an appropriate ratio give almost the same scattering factor as Sr. In this case the Sr/Ca ratio may be less than 2. After many trial calculations, we found that all these cases give nearly the same R_{wp} . We employed, therefore, the model giving a chemical composition, $\text{Bi}_{2.33}\text{Sr}_{1.4}\text{Ca}_{1.3}\text{Cu}_2\text{O}_9$, in which the Sr site is partly occupied by Ca and Bi, and the Ca site is partly occupied by Sr. The composition is consistent with the formation of the Ca_2CuO_3 and CaO impurities, since the nominal composition of the starting material is $\text{Bi}_2\text{Sr}_{1.5}\text{Ca}_{1.5}\text{Cu}_2\text{O}_y$. When the replacement of Ca with Bi instead of Sr was as-

sumed in the above model, the refinement gave $\text{Bi}_{2.3}\text{Sr}_{1.2}\text{Ca}_{1.5}\text{Cu}_2\text{O}_y$ with almost the same R_{wp} . The oxygen sites in the Bi-O layer are occupied with the occupation probabilities less than 1. All of the other sites are fully occupied by a single atom. In particular the Bi site is completely occupied by Bi, though in several models proposed so far, the Bi site is partly occupied by Sr or Cu.^{10,22} Our preliminary calculations based on x-ray and neutron diffraction ruled out such possibilities as mentioned in Sec. V. We assigned isotropic thermal parameters B for all the atoms and neglect their modulations for simplicity. Then we have 8 occupational parameters and 10 thermal parameters. Therefore there are 65 structural parameters together with 23 profile, background, and other parameters for neutron scattering and 16 corresponding parameters for x-ray diffraction and 4 lattice parameters including the \mathbf{b}^* component of the wave vector \mathbf{k} .

The number of isolated peaks is not very large compared with the number of structural parameters because of the overlap of peaks, though we use more than 3500 reflections for neutron and 900 reflections for x-ray diffraction. In particular, almost all the satellite reflections are overlapped with the main reflections. Furthermore, many reflections (about 1000 for neutron and 300 for x ray) give weak intensities less than $\frac{1}{1000}$ of the maximum intensity. (To save the computing time, such reflections were dropped in the calculations of the diffraction pattern and the normal matrix.) Therefore, the structure refinement must be carried out carefully. In fact, we experienced that x-ray scattering and neutron scattering gave different results: the parameters obtained

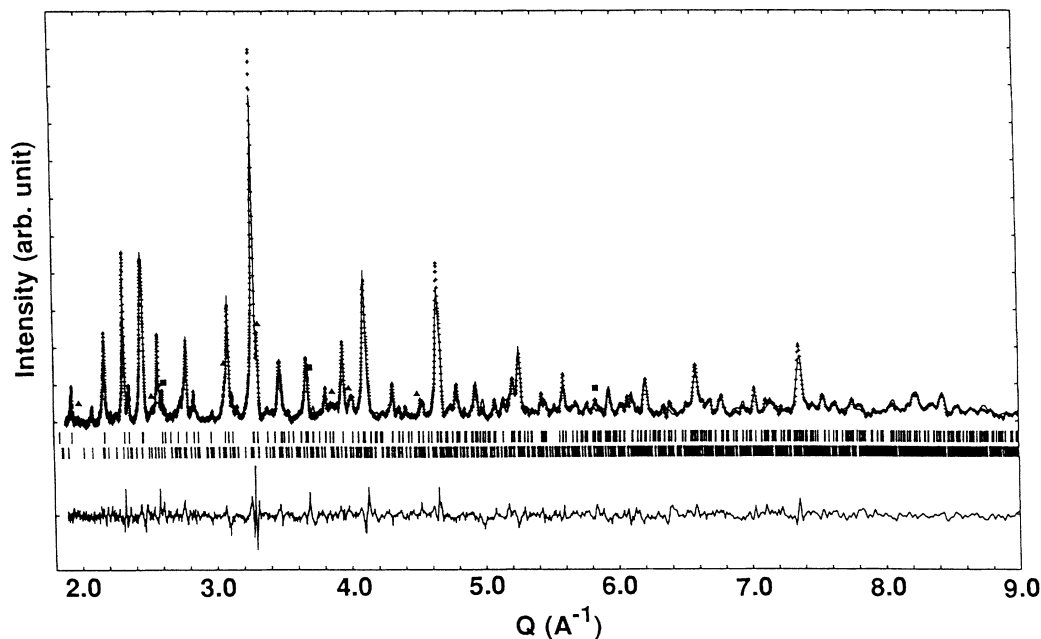


FIG. 2. Observed and calculated neutron-diffraction patterns for $\text{Bi}_2(\text{Sr,Ca})_3\text{Cu}_2\text{O}_{8+x}$. The background is subtracted. The lower solid line represents the difference between the observed and calculated intensities. The vertical bars below the diffraction pattern show the location of the main (upper) and satellite (lower) reflections. Small triangles and squares indicate the positions of strong reflections in Ca_2CuO_3 and CaO, respectively. Peaks at corresponding positions in the difference pattern show the existence of a trace amount of such impurity phases.

from the neutron data gave a very large R factor for the x-ray data. This is considered to be partly due to the poor information included in the powder-diffraction data with heavily overlapped profiles.

In order to avoid obtaining crystallochemically unreasonable results, we use the penalty functions that restrict interatomic distances and occupation probabilities within reasonable ranges.¹⁶ The penalty functions have the same form as in REMOS. We restricted the interatomic distances between two metals (Bi and Cu) and oxygens around them forming square pyramids. Allowed ranges of the interatomic distances used in the analysis are listed in Table III. This restrains the appearance of Bi—O and Cu—O lengths less than 2.0 and 1.8 Å, respectively, while their upper limit (3.5 Å) is large enough so that it gives no restriction practically. The penalty function for the occupation probability suppresses the appearance of a nonphysical probability less than 0 or greater than 1.

IV. MODULATED STRUCTURE

The modulated structure was refined with equal weights for x-ray and neutron data: we minimized $[R_{wp}(x \text{ ray})]^2 + [R_{wp}(\text{neutron})]^2 + P^2$. After a number of cycles, the final result gave small R factors and a small penalty function, which implies that a crystallochemically reasonable result could be obtained. The final R_{wp} is 0.090 for x ray diffraction and 0.092 for neutron diffraction. These are not very small because of the existence of the impurity phases and the irregular change in FWHM due to the intergrowth. The final profile fit and difference patterns for neutron and x-ray scattering are shown in Figs. 2 and 3. The absorption effect and the Q dependence of the efficiency of counters are corrected in Fig. 2. The intensity of each line is proportional to the

integrated value of the profile shape function times the geometrical factor Q^{-2} . Figure 3 is the usual plot without Lorentz and polarization correction. (In order to improve the signal-to-noise ratio of the data, the intensity data were filtered with a low-pass filter using the fast Fourier transformation. This improved R_{wp} by the order of 0.01 and therefore may be efficient for extracting the information of the modulation included in the weak satellite reflections.)

The lattice parameters of the average structure were refined to be $a = 5.3957(3)$, $b = 5.3971(3)$, $c = 30.649(1)$ Å, and $\mathbf{k} = 0.2118(1)\mathbf{b}^*$. The preferred orientation parameters were $p_1 = 0.89$ and $p_2 = 2.69$ for the x-ray data and $p_1 = 0$ and $p_2 = 0.26$ for the neutron data. Final structural parameters are shown in Table IV. The amplitude of the sine wave in the Bi displacement to the b direction is positive. This means that Bi is dilute at $t \approx 0$ and condensed at $t \approx \frac{1}{2}$. The refined occupation probabilities give the chemical composition $\text{Bi}_{2.3}\text{Sr}_{1.4}\text{Ca}_{1.3}\text{Cu}_2\text{O}_9$, which is quite reasonable from the composition of the starting material and the coexistence of a minor amount of Ca_2CuO_3 and CaO . However, the number of the extra oxygen per f.u. is very large (1.0) compared with that in the previous reports (0.15–0.25).^{3,6} Therefore we made again the structure refinement of a model with no extra oxygen starting with the final positional parameters. In this model the occupation probabilities of O(5) and O(6) are zero and that of O(4) is 1. The model gave $R_{wp} = 0.115$ (0.096) for the neutron (x-ray) data and the extremely large isotropic thermal parameter of $B = 15 \text{ \AA}^2$ for O(4), indicating that the O(4) site is partly deficient. When the model with 0.4 extra oxygen per f.u. was employed, R_{wp} dropped to 0.098 (0.092) and the thermal parameter of O(4) was 7 \AA^2 . The final results, $R_{wp} = 0.092$ (0.090), are clearly better than these. However, the large

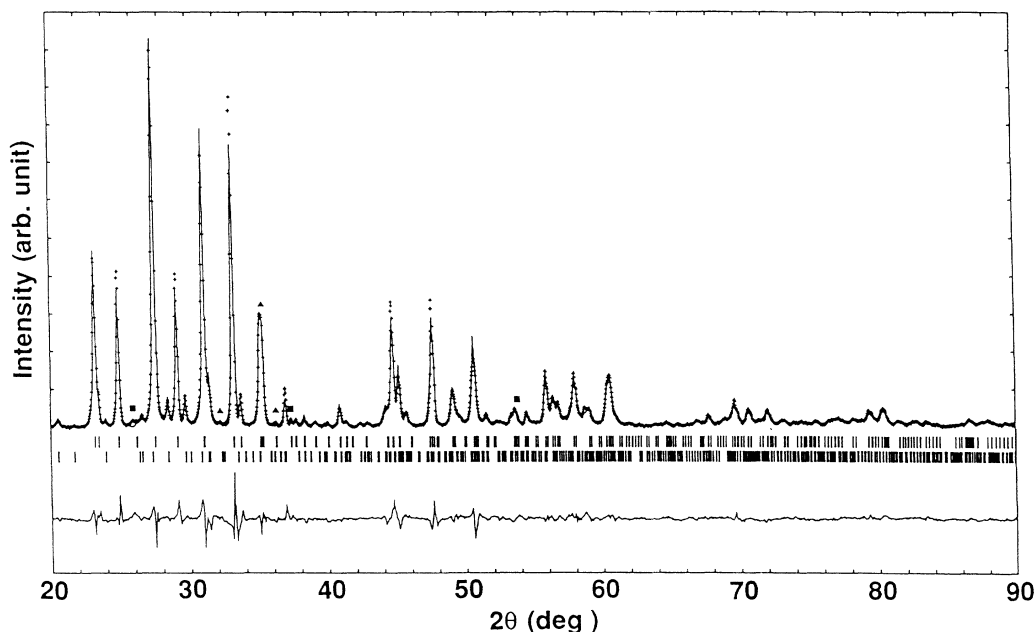


FIG. 3. Observed and calculated x-ray-diffraction patterns for $\text{Bi}_2(\text{Sr,Ca})_3\text{Cu}_2\text{O}_{8+x}$. The meanings of lines and symbols are the same as in Fig. 2. The contribution from Ca_2CuO_3 and CaO to the intensity is also visible in the difference pattern.

TABLE IV. The structural parameters of the modulated structure. The third column (corresponding to 1 in the heading) represents the parameters for the average structure. The fourth and fifth columns are the amplitudes for the cosine and sine waves. The last three columns are the corresponding values by Gao *et al.* (Ref. 7). The values have been multiplied by 10^4 for positional parameters and 10^2 for thermal parameters (\AA^2) and occupational ones. The standard deviations are in parentheses. [A common thermal parameter is assumed for O(5) and O(6).] a, b, and c: occupation probabilities of Bi, Ca, and Sr. The standard deviations are estimated from the formula $\sigma(p_i) = [A_i^{-1} M_p / (N_b - P_c)]^{1/2}$, where the meaning of symbols are the same as that in Ref. 25.

Atom		Present work			Gao <i>et al.</i>		
		1	cos(2 πt)	sin(2 πt)	1	cos(2 πt)	sin(2 πt)
Bi	x	2273(14)	-100(35)		2285	-74	
	y	5000		745(15)	5000		721
	z	520(1)	-52(2)		522	-61	
	B	152(17)					
	p	100	0		100		
Sr	x	2500(30)	161(65)		2537	137	
	y	0		365(36)	0		444
	z	1401(2)	-91(5)		1409	-65	
	B	139(33)					
	p	50(18)	-45(21)		100		
a	p	15(10)	9(12)				
b	p	35(10)	36(12)				
Ca	x	2500	142(97)		2500	0	
	y	0			0		
	z	2500	-99(8)		2500	0	
	B	24(41)					
	p	60(4)					
c	p	40(4)					
Cu	x	2477(29)	142(58)		2498	0	
	y	5000		94(34)	5000		74
	z	1955(3)	-102(4)		1967	-91	
	B	42(21)					
	p	100			100		
O(1)	x	0		40(68)	0		
	y	2500		-200(77)	2500		
	z	1964(9)	-74(18)		1950		
	B	81(61)					
	p	100			100		
O(2)	x	5000		216(61)	5000		
	y	2500		173(69)	2500		
	z	1979(8)	-97(15)		2020		
	B	-20(54)					
	p	100			100		
O(3)	x	2131(60)	-545(93)		2800		
	y	5000		945(75)	5000		
	z	1166(6)	-58(11)		1220		
	B	175(54)					
	p	100			100		
O(4)	x	1612(140)	198(197)		1500		
	y	0		1280(104)	0		
	z	517(35)	-103(45)		530		
	B	-119(72)					
	p	48(3)	-53(3)		100		
O(5)	x	5000		-1620(181)			
	y	2500		-312(164)			
	z	603(66)	-311(83)				
	B	659(169)					
	p	52(3)	53(3)		0		
O(6)	x	0		-1324(181)			
	y	2500		2337(210)			
	z	462(65)	281(92)				
	B	659(169)					
	p	52(3)	53(3)		0		

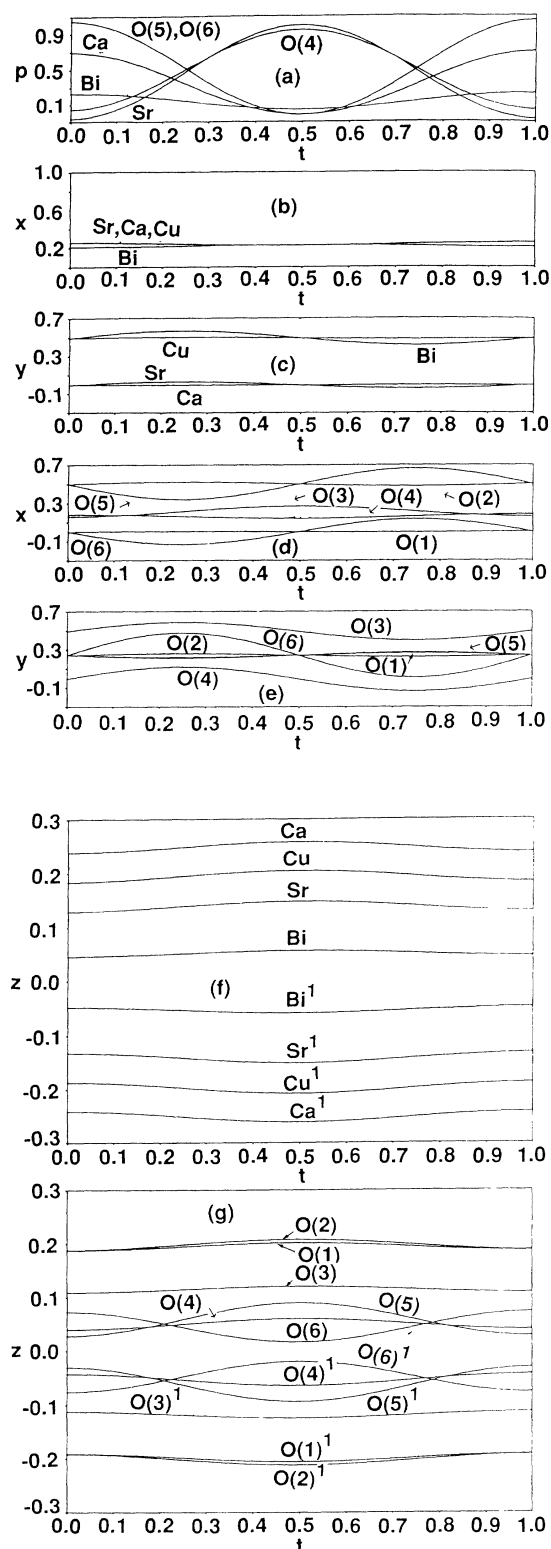


FIG. 4. Modulation waves of the occupational and displacive modulations. (a) The occupation probabilities of the metal atoms at the Sr site and of the O(4), O(5), and O(6) sites. (b) and (c) the x and y coordinates of metal atoms. (d) and (e) x and y coordinates of oxygen atoms. (f) and (g) the z coordinates of metal and oxygen atoms. M^1 or $O(i)^1$ means the atom obtained from metal M or oxygen $O(i)$ by the symmetry operation $-x, y, -z$.

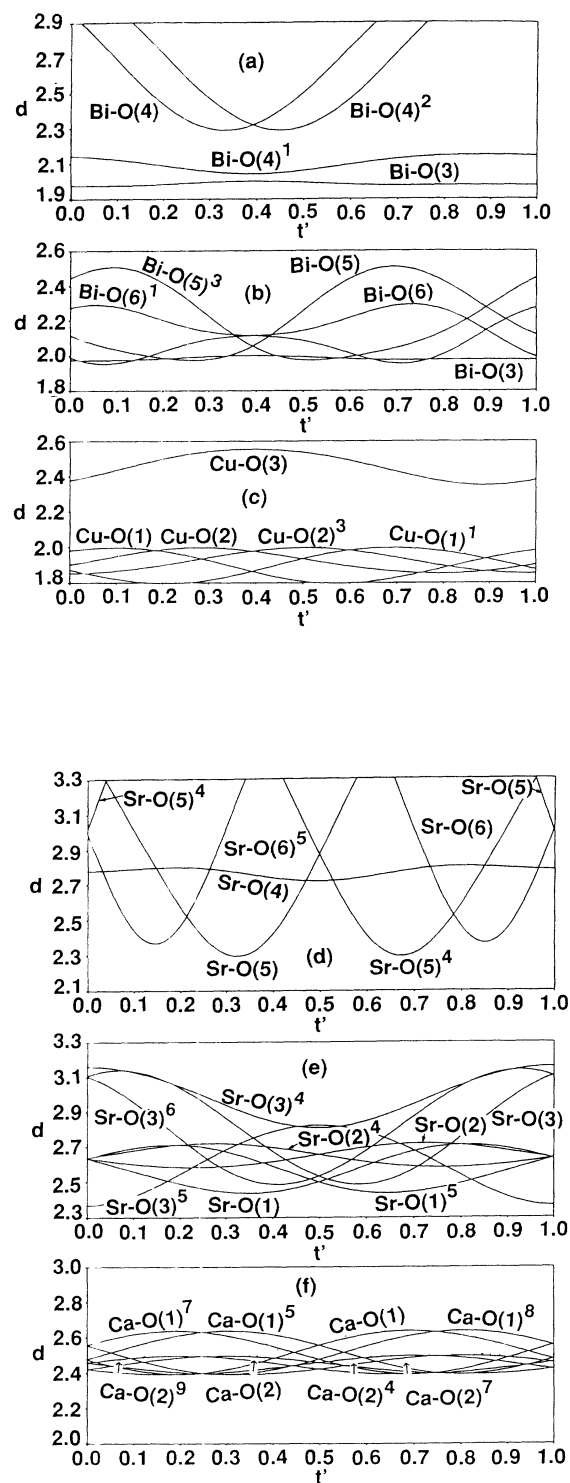


FIG. 5. Metal—oxygen distances (in Å) as a function of $t' = t - \mathbf{k} \cdot \bar{\mathbf{x}}$. (a) Bi—O(3,4); (b) Bi—O(3,5,6); (c) Cu—O; (d) Sr—O to the oxygens in the Bi—O layer; (e) Sr—O to the oxygens in the Sr—O and Cu—O layers; (f) Ca—O. $O(i)^j$ means the atom obtained from $O(i)$ by the j th symmetry operation shown below.
 1: $-x, y + \frac{1}{2}, z$; 2: $x, y + 1, z$; 3: $-x + 1, y + \frac{1}{2}, z$;
 4: $-x + 1, y - \frac{1}{2}, z$; 5: $-x, y - \frac{1}{2}, z$; 6: $x, y - 1, z$;
 7: $-x + \frac{1}{2}, y, -z + \frac{1}{2}$; 8: $x + \frac{1}{2}, y - \frac{1}{2}, -z + \frac{1}{2}$;
 9: $x - \frac{1}{2}, y - \frac{1}{2}, -z + \frac{1}{2}$.

thermal parameters of O(5)–O(6), 6.6 \AA^2 , may suggest a slightly smaller number of extra oxygens is probable. In order to check this, we refined the structure again with fixing the thermal parameter at $B = 2 \text{ \AA}^2$ for these atoms. Then the occupation probabilities of O(5)–O(6) reduces from 0.52 to 0.49. This change is negligibly small. Furthermore, we checked the change in the occupation probabilities of O(4)–O(6) when the constraints between their occupation probabilities are released, expecting the decrease in the total occupation probability. However, the occupation probabilities of O(5) and O(6) increased with the increase in their thermal parameters, while that of O(4) was almost unchanged. This is considered to be due to the correlation of the occupation probability and the thermal parameter. This model is not natural because the sum of the occupation probabilities of O(4) and O(5) or O(6) exceeds one and the interatomic distance of them is very short (see Fig. 1). Consequently, all the attempts failed to find less extra oxygen atoms. The present analysis therefore concludes that one extra oxygen per f.u. is the most probable.

Several thermal parameters were negative because of the difficulty in determining them by powder diffraction. The modulation waves for the displacive and occupational modulations are shown in Fig. 4 and the interatomic distances of metal and oxygen are given in Fig. 5.

Figure 4(a) shows that the O(4) site in the Bi–O layer is almost fully occupied near $t = \frac{1}{2}$, while the O(5) and O(6) sites have large occupation probabilities near $t = 0$. This clearly shows that BiO_5 pyramids form the Bi-dilute regions (see Fig. 1). In the Sr site, Bi and Ca are located at

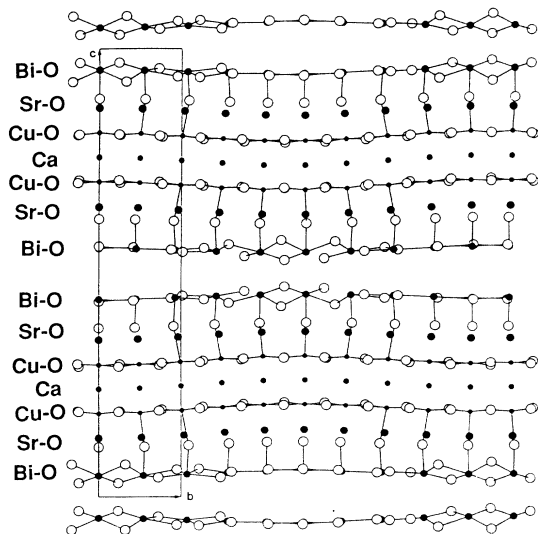


FIG. 6. The projection of the modulated structure of $\text{Bi}_2(\text{Sr,Ca})_3\text{Cu}_2\text{O}_{8+x}$ along the a axis. Solid and open circles represent metal and oxygen atoms. The solid box is the outline of the unit cell. The five cells along the b direction are plotted, which correspond nearly to the one modulation period. The Cu–O bonds shorter than 2.5 \AA and the Bi–O bonds shorter than 2.7 \AA are plotted. The figure shows that some Cu–O bonds to the apical oxygens of the CuO_5 pyramid are longer than 2.5 \AA .

$t \approx 0$, and Sr at $t \approx \frac{1}{2}$. (In the Ca site, Sr is randomly distributed because of the site symmetry. See Tables I and II.)

The displacements of metal atoms along the a axis are small compared with those of Bi atoms along the b axis [Figs. 4(b) and 4(c)], while O(3)–O(6) move largely to one of these or to both directions [Figs. 4(d) and 4(e)]. It is noted that these oxygen atoms are all situated around Bi atoms. This means that oxygen arrangements around the Bi atoms are considerably distorted from those of the fundamental structure. Figures 4(f) and 4(g) indicate displacements along the c axis. As is clear from the figure, adjacent Ca, Cu, and Sr layers move by almost the same amount along the same direction, while O(5) and O(6) layers are markedly displaced along the opposite direction to each other.

Figures 5(a) and 5(b) indicate that in the Bi-dilute region ($0 < t' < 0.15$, $0.65 < t' < 1$), Bi has five Bi–O bonds shorter than 2.55 \AA , while it has four in the Bi-condensed region ($0.15 < t' < 0.65$). [Note that O(4) has a large occupation probability in the latter, while the probabilities for O(5) and O(6) are large in the former. See Fig. 4(a).]

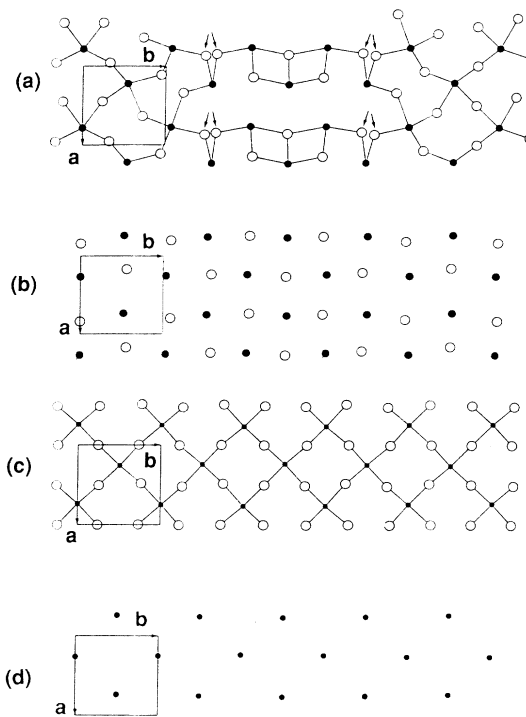


FIG. 7. The projection of metal and metal-oxygen layers normal to the c axis. (a) The Bi–O layer at $z \approx 0.06$; (b) the Sr–O layer at $z \approx 0.14$; (c) the Cu–O layer at $z \approx 0.2$; (d) the Ca layer at $z \approx \frac{1}{4}$. Solid and open circles represent metal and oxygen atoms. The Cu–O bonds shorter than 2.5 \AA and the Bi–O bonds shorter than 2.7 \AA are plotted. The oxygen atoms in the Bi–O layer have the occupational modulation, so that the oxygens with the occupation probability greater than 0.4 are drawn. The arrows show that the statistically occupied two positions with the occupation probability near $\frac{1}{2}$. The figure shows that there are four Bi–O bonds for each Bi within the plane of the Bi-dilute region while three bonds exist in the Bi-condensed region.

Cu has four short bonds ($\cong 1.9 \text{ \AA}$) on the Cu-O layer and one longer bond ($\cong 2.5 \text{ \AA}$) to the apical oxygen O(3) of the pyramid [Fig. 5(c)]. The Cu—O(3) lengths change considerably, owing to the large displacements of O(3) atoms that are bonded to Bi. The bond distances of Sr and Ca to the neighboring O also change markedly [Figs. 5(d)–5(f)].

The projection of the modulated structure along the a axis is shown in Fig. 6. Since the period of the modulation wave is about $4.8b$, the range within $5b$ is drawn. The characteristic feature of the structure is the existence of strong displacive modulations for all the atoms. In particular, atoms on the Bi-O layers move largely in the b direction, while those on the Cu-O and Ca layers are displaced mainly parallel to the c axis. Sr moves in both directions. The displacements of Sr and Ca along the c axis are almost the same as that of Cu, while the Bi movement in this direction is small as mentioned before. The apical oxygen O(3) of the CuO_5 square pyramid moves along with Bi in the b direction, but the displacement along the a axis is also large as shown in Fig. 4(d). As a result the CuO_5 pyramid distorts. This suggests that the apical oxygen is bonded firmly to Bi rather than Cu, while the four bonds in the Cu layer are tight. In fact the Bi—O(3) bond is much shorter than the Cu—O(3) bond [Figs. 5(a) and 5(c)]. The displacements of metal atoms are consistent with those observed by electron microscopy.^{10,13}

Figure 7 shows the projection of each layers within $0 < z < \frac{1}{4}$ along the c axis. As is seen in Figs. 7(c) and 7(d), the Cu-O and Ca layers are almost regular. This and Fig. 6 show that the main movement of the Cu-O layer is the bending of the layer and the slight rotation of CuO_4 parallel to the c axis, leaving the oxygen square almost unchanged. In the Sr-O layer [Fig. 7(b)], the Sr atoms are arranged almost regularly but make slightly condensed and dilute regions because of the displacement along the b axis. (This is more clearly seen in Fig. 6.) The O(3) atoms move markedly in both the a and b directions. The structure of the Bi-O layer [Fig. 7(a)] is complicated because it consists of two different structures: Bi has different oxygen arrangements in the Bi-condensed and Bi-dilute regions. They are alternated with the periodicity of the modulation wave. Therefore, oxygen atoms with occupation probabilities larger than 0.4 are plotted in the figure. In the Bi-condensed region (center), each Bi atom has four short bonds, three within the Bi-O layer and one to the apical oxygen of the CuO_5 square pyramid [Figs. 6 and 7(a)]. On the other hand, the Bi-dilute region (right and left ends) has distorted BiO_5 square pyramids. The pyramids greatly rotate about the c axis owing to the large displacements of O(5) and O(6) in order to connect with a quite different oxygen arrangement in the Bi-condensed region. The rotation angle periodically changes along the b axis. The change in the coordination number of oxygen in the Bi-O layer affects the oxygen coordination around Sr. Sr has twelvefold oxygen coordination over (or underneath) the Bi-dilute region if O(3), O(5), and O(6) do not move, but the large displacements of them reduce the coordination number to 6 or 7. On the other hand, of the nine oxygen atoms neighboring Sr

over the Bi-condensed region, three give Sr—O distances longer than 2.7 \AA . In particular, the interatomic distances from Sr to the oxygen atoms on the Sr-O layer change considerably as shown in Fig. 7(b).

This structure has the extra oxygen atoms because of the presence of the square pyramidal BiO_5 . From the average occupation probabilities of O(4), O(5), and O(6), x in the chemical formula is about 1.0. This value is in good agreement with those determined by specific gravity ($x = 0.92$) and the inert gas fusion method ($x = 0.73$).²⁰

V. DISCUSSION

Since the discovery of $\text{Bi}_2(\text{Sr,Ca})_3\text{Cu}_2\text{O}_{8+x}$, the causes of the modulated structure are extensively discussed based on x-ray single-crystal diffraction, x-ray and neutron powder diffraction and electron microscopy. The origins of the modulation proposed so far are classified into the three types: (1) a partial substitution of Sr or Cu for Bi,^{10,22} (2) ordering of Sr vacancies,²³ and (3) insertion of the extra oxygen in the Bi-O layer.^{13,14} The present analysis clearly showed the existence of the extra oxygen and this is the reason for the occurrence of the modulation, though the extra-oxygen content does not agree with the values in the previous studies and the discrepancy remains to be unsolved. We, however, checked other possibilities to confirm this view. In order to check the first case, the occupation probability of Bi was refined. Such substitution may give an average occupation probability less than 1 because the atomic scattering factor for x ray and scattering length for neutron diffraction of Bi are the largest of all the metals. The result of the refinement gave an occupation probability slightly larger than 1 ($p = 1.02$), indicating that the Bi site is fully occupied only by Bi. The second point is more delicate because it is difficult to distinguish slight deficiency of the Sr site from the partial substitution of Ca for Sr. In the calculation, the latter was assumed and the occupation probabilities of Ca and Sr were refined. The occupation factor of Ca was the order of 0.05. Therefore even if the Sr vacancies exist, their ratio is the order of 0.025. This value is too small to explain the strong modulation of this structure. Thus the first two possibilities are ruled out by the present analyses.

The present results are consistent with a structural model for $\text{Bi}_2\text{Sr}_{2.4}\text{Y}_{0.6}\text{Cu}_2\text{O}_{8+x}$ proposed by Torardi *et al.*,¹⁴ who confirmed the presence of the extra oxygen. That is, O(5) and O(6) in the Bi-dilute region take roughly the same oxygen positions as in their model for $\text{Bi}_2\text{Sr}_{2.4}\text{Y}_{0.6}\text{Cu}_2\text{O}_{8+x}$. In this model, the oxygen atoms on the Bi-O layer are largely displaced from "ideal positions" called by them, forming Bi—O chains along the direction of the modulation [upper two chains and extra oxygen atoms in Fig. 3(c) in Ref. 14]. However, the O(4) atom in the Bi-condensed region occupy rather the ideal position [Fig. 3(a) of Ref. 14].

Finally we compare our results to those of Gao *et al.*, obtained by single-crystal x-ray diffraction.⁷ In their work, the modulated structure was analyzed based on the same superspace group as in the present analysis. They clarified the modulation waves of metal atoms, using up to the second-order harmonics in the modulation waves

for the analysis with main and first-order satellite reflections. The modulation waves are quite different from the present ones and results obtained by electron microscopy.^{10,13} The main difference is present in the large second-order harmonics. Since it is quite difficult to determine the second-order Fourier amplitudes from the main and first-order satellite reflections, we cannot understand their meaning. (We believe that the second-order Fourier amplitudes should be excluded in the refinement when the second-order satellite reflections are not available because they contribute mainly to the second-order satellite intensities. See also Ref. 24.) Therefore the parameters for the average structure and the first-order Fourier amplitudes by Gao *et al.* are listed in Table IV together with the present results for comparison. As is clearly from the table, the agreement of Fourier amplitudes is poor, in particular for Ca and Cu. Ca moves largely along the *c* axis in the present result while no displacement is shown by Gao *et al.*, and Sr, Ca, and Cu move by almost the same amount along the *a* axis in the present work, while displacements of Ca and Cu larger than their standard deviations are not detected in the result of Gao *et al.* However, we have to consider that the standard deviations in the Rietveld method do not take into account the overlap of the line profile in the diffraction pattern and as a result they are underestimated in general. Even if such a situation is taken into account, the discrepancy in the Fourier amplitude of the displacement in Ca along the *c* axis will still remain. The disagreement will partly be due to the difference in crystals but may partly be due to the difficulty in an analysis by the single-crystal method as mentioned at the beginning. It is expected that the discrepancy is removed in

the near future by the refinement with a high-quality sample.

VI. CONCLUSION

The present analysis clarified the complicated modulated structure of the superconducting oxide $\text{Bi}_2(\text{Sr,Ca})_3\text{Cu}_2\text{O}_{8+x}$ by using the newly developed Rietveld refinement program and the simultaneous refinement method with x-ray and neutron-powder-diffraction data. This method is quite effective for analyzing the modulated structure giving the satellite reflections strong enough to be detectable by the powder method. The characteristic feature of the modulated structure is the existence of the extra oxygen atoms on the Bi-O layer. The extra oxygen atoms increase the Bi—Bi distance, creating the Bi-condensed and Bi-dilute regions alternately along the *b* axis. According to the displacement of Bi, the apical oxygen of the CuO_5 pyramid moves along with Bi and the pyramid is distorted. The displacements of Sr and Ca are accompanied by the distortion. Over (or underneath) the Bi-dilute region, the Sr site is occupied by Bi and Ca, while over the Bi-condensed region it is occupied by Sr. The Ca site is randomly occupied by Sr. From the above results we conclude that the existence of the extra oxygen atoms on the Bi-O layer is the main origin of the modulated structure and the extra oxygen plays a role of the hole dopant, which is considered to be essential in superconductivity. (We have recently become aware of a paper by Lee *et al.*²⁶ that reports that the Ca and Sr sites are partly occupied by Bi.)

ACKNOWLEDGMENTS

We wish to thank Dr. A. Ono, National Institute for Research in Inorganic Materials, for helpful discussions.

- ¹H. Maeda, Y. Tanaka, M. Fukutomi, and T. Asano, *Jpn. J. Appl. Phys.* **27**, L209 (1988).
- ²A. Ono, S. Sueno, and F. P. Okamura, *Jpn. J. Appl. Phys.* **27**, L786 (1988).
- ³J. M. Tarascon, Y. Le Page, P. Barboux, B. G. Bagley, L. H. Greene, W. R. McKinnon, G. W. Hull, M. Giroud, and D. M. Hwang, *Phys. Rev. B* **37**, 9382 (1988).
- ⁴M. A. Subramanian, C. C. Torardi, J. C. Calabrese, J. Gopalakrishnan, K. J. Morrissey, T. R. Askew, R. B. Flippen, U. Chowdhry, and A. W. Sleight, *Science* **239**, 1015 (1988).
- ⁵K. Imai, I. Nakai, T. Kawashima, S. Sueno, and A. Ono, *Jpn. J. Appl. Phys.* **27**, L1661 (1988).
- ⁶S. A. Sunshine, T. Siegrist, L. F. Schneemeyer, D. W. Murphy, R. J. Cava, B. Batlogg, R. B. van Dover, R. M. Fleming, S. H. Glarum, S. Nakahara, R. Farrow, J. J. Krajewski, S. M. Zahurak, J. V. Waszczak, J. H. Marshall, P. Marsh, L. W. Rupp, Jr., and W. F. Peck, *Phys. Rev. B* **38**, 893 (1988).
- ⁷Y. Gao, P. Lee, P. Coppens, M. A. Subramanian, and A. W. Sleight, *Science* **241**, 954 (1988).
- ⁸M. Onoda and M. Sato, *Solid State Commun.* **67**, 799 (1988).
- ⁹Y. Matsui, H. Maeda, Y. Tanaka, and S. Horiuchi, *Jpn. J. Appl. Phys.* **27**, L372 (1988).
- ¹⁰S. Horiuchi, H. Maeda, Y. Tanaka, and Y. Matsui, *Jpn. J. Appl. Phys.* **27**, L1172 (1988); Y. Hirotsu, O. Tomioka, T. Ohkubo, N. Yamamoto, Y. Nakamura, S. Nagakura, T. Komatsu, and K. Matsushita, *ibid.* **27**, L1869 (1988).
- ¹¹H. G. von Schnering, L. Walz, M. Schwarz, W. Becker, M. Hartweg, T. Popp, B. Hettich, P. Müller, and G. Kämpf, *Angew. Chem. Int. Ed. Engl.* **27**, 574 (1988).
- ¹²P. Bordet, J. J. Capponi, C. Chaillout, J. Chenavas, A. W. Hewat, E. A. Hewat, J. L. Hodeau, M. Marezio, J. L. Tholence, and D. Tranqui, *Physica C* **156**, 189 (1988).
- ¹³H. W. Zandbergen, W. A. Groen, F. C. Mijlthoff, G. van Tendeloo, and S. Amelinckx, *Physica C* **156**, 325 (1988).
- ¹⁴C. C. Torardi, J. B. Parise, M. A. Subramanian, J. Gopalakrishnan, and A. W. Sleight, *Physica C* **157**, 115 (1989).
- ¹⁵A. Yamamoto, A. Computer Program for the Refinement of Modulated Structures REMOS 82.0, National Institute for Research in Inorganic Materials (1982) (unpublished); A. Yamamoto, *Acta Crystallogr. Sec. A* **38**, 87 (1982).
- ¹⁶A. Yamamoto, H. Nakazawa, M. Kitamura, and N. Morimoto, *Acta Crystallogr. Sec. B* **40**, 228 (1984).
- ¹⁷F. Izumi, *Nippon Kessho Gakkaishi, J. Crystallogr. Soc. Jpn.* (in Japanese) **27**, 23 (1985); F. Izumi, H. Asano, H. Murata, and N. Watanabe, *J. Appl. Crystallogr.* **20**, 411 (1987).
- ¹⁸M. Onoda, A. Yamamoto, E. Takayama-Muromachi, and S. Takekawa, *Jpn. J. Appl. Phys.* **27**, L833 (1988).
- ¹⁹J. Q. Li, C. Chen, D. Y. Yang, F. H. Li, Y. S. Yao, Z. Y. Ran, W. K. Wang, and Z. X. Zhao, *Z. Phys. B* **74**, 165 (1989).

- ²⁰E. Takayama-Muromachi, Y. Uchida, A. Ono, F. Izumi, M. Onoda, and Y. Matsui, *Jpn. J. Appl. Phys.* **27**, L365 (1988).
- ²¹A. Yamamoto, *Acta Crystallogr. Sec. B* **38**, 1446 (1982).
- ²²T. Kajitani, K. Kusaba, M. Kikuchi, N. Kobayashi, Y. Syono, T. B. Williams, and M. Hirabayashi, *Jpn. J. Appl. Phys.* **27**, L587 (1988).
- ²³A. K. Cheetham, A. M. Chippindale, and S. J. Hibble, *Nature* (London) **21**, 333 (1988).
- ²⁴S. van Smaalen and K. D. Bronsema, *Acta Crystallogr. Sec. B* **42**, 43 (1986).
- ²⁵H. G. Scott, *J. Appl. Crystallogr.* **16**, 156 (1983).
- ²⁶P. Lee, Y. Gao, H. S. Sheu, V. Petricek, R. Restori, P. Coppens, A. Darovskikh, J. C. Phillips, A. W. Sleight, and M. A. Subramanian, *Science* **244**, 62 (1989).